Systemic Chemistry

Selective Coordination Bonding in Metallo-Supramolecular Systems on Surfaces**

Alexander Langner, Steven L. Tait,* Nian Lin, Rajadurai Chandrasekar, Velimir Meded, Karin Fink, Mario Ruben,* and Klaus Kern*

The confinement of molecular species in nanoscale environments strongly modifies the interaction pathways compared to homogenous, three-dimensional (bulk) conditions. A new field of chemistry featuring weak interactions, coordination bonding, and covalent chemistry at solid surfaces has recently emerged.[1–8] In particular, the combination of surface-confined chemistry and scanning probe techniques with sub-nanometer resolution allows immediate insights into molecular self-organization processes on the nanometer level. Extended monolayers of open, two-dimensional (2D) coordination networks with high organizational periodicity, controlled symmetries, and modular dimensionality have been achieved by using designed, self-instructed molecular building blocks.[9]
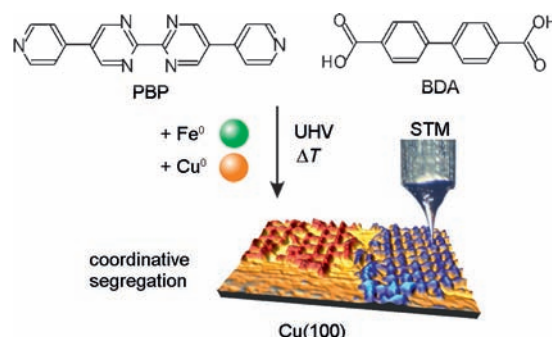
The deposition of mixtures of precursor molecules has led to more sophisticated architectures, mainly built on weak intermolecular interactions[10–14] or weak interactions in combination with coordination bonding, that is, hierarchical motifs.[15,16] The cooperative assembly of instructed mixtures of molecular bricks enables a high degree of structural control and functionality, for example, the stability and ordering of primary structures can be increased,[15] or the dimensionality and geometry of supramolecular structures can be steered.[16–18] Observations of molecular-level self-recognition and error correction have demonstrated collective dynamics in surface-confined supramolecular systems.[11,18]

A grand challenge in materials chemistry is the capability to design adaptive materials, that is, to develop systemic methods for tailored structure and function. To exploit the opportunities of systemic chemistry, a detailed understanding of the selectivity in the interaction mechanisms of molecular mixtures, if possible by direct studies at the single-molecule level, is of pivotal interest.

Herein, we report on the observation of supramolecular selectivity in the simultaneous coordinative interaction of two different molecular ligands, aromatic bipyrimidines and dicarboxylic acids, with Cu and Fe atoms resulting in a self-segregation into two distinct, surface-confined coordination network domains. The random mixture of ligands and metals separates into subdomains of pure bipyrimidine–Cu and carboxylate–Fe networks, while heteroleptic ligand combinations, though feasible, are not observed. Each 2D coordination network exhibits a tetragonal geometry with metal atom coordination nodes, but expresses unique molecular composition and spatial organization.

The molecular components PBP (5,5′-bis(4-pyridyl)(2,2′-bipyrimidine)) and BDA (1,4′-biphenyl-dicarboxylic acid, see Scheme 1) are co-evaporated in a 1:1 number ratio onto a Cu(100) substrate at room temperature under ultra-high vacuum (UHV) conditions. At this temperature, a diffusing copper adatom gas is present at the Cu(100) surface, which has been shown to be available for the formation of extended

[*] A. Langner, Prof. Dr. S. L. Tait, Prof. Dr. N. Lin, Prof. Dr. K. Kern
Max Planck Institute for Solid State Research
Heisenbergstraße 1, 70569 Stuttgart (Germany)
E-mail: tait@indiana.edu
K.Kern@fkf.mpg.de

Prof. Dr. S. L. Tait
Department of Chemistry, Indiana University
Bloomington, IN 47405 (USA)

Prof. Dr. N. Lin
Department of Physics
The Hong Kong University of Science and Technology
Clear Water Bay, Kowloon, Hong Kong (China)

Prof. Dr. R. Chandrasekar, Dr. V. Meded, Dr. K. Fink,
Prof. Dr. M. Ruben
Institute of Nanotechnology, Research Center Karlsruhe
PF 3640, 76021 Karlsruhe (Germany)
E-mail: mario.ruben@kit.edu

Prof. Dr. R. Chandrasekar
School of Chemistry, University of Hyderabad
Central University Post, Gachibowli, Hyderabad-500046 (India)

Prof. Dr. M. Ruben
IPCMS-CNRS, Université de Strasbourg
23, rue de Loess, 67034 Strasbourg (France)

Prof. Dr. K. Kern
Institute de Physiques de la Matière Condensée, Ecole Polytechnique Fédérale de Lausanne, 1015 Lausanne (Switzerland)

Supporting information for this article is available on the WWW under http://dx.doi.org/10.1002/anie.201108530.

Scheme 1. Representation of the linear, parallel readout of two coordination algorithms from the instructed mixture of two ligands and two metal species confined on a Cu(100) surface.

coordination architectures.[19, 20] Subsequently, the temperature is increased to 450 K and the second metal, zero-valent iron, is deposited onto the "hot" substrate. The subsequent annealing process serves multiple purposes: 1) it assures deprotonation of the carboxylic acid groups of BDA, forming carboxylate functionalities,[21, 22] 2) it enables effective reversibility of preformed bonding interactions,[18] 3) it provides thermal energy to activate the less-stable bonds that would otherwise lead to disordered or entropic structures, and 4) it causes an increase in the mobility (2D diffusivity) of the elementary building blocks. In consequence, the annealing process dissolves initial, kinetic assemblies (usually disordered and trapped by low mobility) and induces a dynamic redistribution of the molecular building blocks PBP, BDA, Cu, and Fe. The building blocks have sufficient mobility at this temperature to sample available bonding sites, and the system can thereby progress toward a thermodynamically favored configuration.

The randomly distributed reaction mixture is allowed to cool to room temperature, and supramolecular segregation into subdomains is observed in high-resolution STM topographs (Figure 1a). The selective formation of two different types of 2D coordination networks with distinct geometries can be distinguished: 1) a highly regular network with tetragonal symmetry exhibiting a pore size of 12 Å (marked by blue arrow, Figure 1a) and 2) a more flexible network with

Figure 1. a) High-resolution STM image of the self-assembly of PBP, BDA, Fe, and Cu, starting from an initial random distribution of the building blocks. The STM image displays two types of networks (room temperature, 40 nm × 25 nm). Copper selectively coordinates with PBP (blue arrow, model in (b)) and iron selectively coordinates with BDA (white arrows, model in (c)). Color codes: Fe green, Cu yellow, N blue, O red.

larger cavities exhibiting between 20 and 25 Å pore size (marked by white arrows, Figure 1a).

The first network of smaller pore size forms large domains with extensions of 200 to 400 nm^2 and a lattice periodicity of 23 Å (marked by blue arrow, Figure 1a). The observed structure matches prior studies of PBP–Cu networks of $[Cu_4(PBP)_2]_n$ constitution on the same substrate (see Figure 1b).[23] Structurally, the network is constructed from a three-fold coordination motif around the copper atoms. Each copper atom is coordinated by three nitrogen electron-donor atoms of PBP: two donor atoms coordinate as bipyrimidine chelate of one PBP molecule, while the third donor atom is the terminal pyridyl group of a second PBP molecule (Figure 1b). The coordination sphere around the copper atom can be described, within the limits of STM resolution, as trigonal planar, but an additional metal–metal contact to the underlying substrate cannot be excluded.[24] The charge state of the Cu center cannot be unambiguously determined from the coordination geometry and character of the ligating species, owing to the possible charge transfer to and charge compensation by the underlying metal surface (see the Supporting Information for further discussion of this point).

The second network consists of coexisting structural adaptations of an orthogonal BDA–Fe network (marked by white arrows, Figure 1a), which has also been reported.[25] This network is stabilized by Fe–O bonds to produce a periodic $[Fe_4(BDA)_4]_n$ constitution, whereby dimeric iron coordination centers are stabilized by two bridging μ-carboxylates. The coordination sphere is completed by two non-bridging, monodentate carboxylates (see Figure 1c). The observed structural diversity is introduced by different orientations of Fe–Fe axes on the surface. The dimeric coordination motif has been proven to be robust in various bis(carboxylate) systems with iron and cobalt.[25, 26]

In principle, the non-bridging monodentate carboxylate groups in the Fe–BDA motif can be replaced with pyridine functionalities, which satisfy maximal site occupancy and form stable coordination nodes at room temperature.[27] We reported recently a regular ladder-type architecture that is based on this coordination motif, which is formed by a very similar mixture, that is, iron, BDA, and linear polyphenyls with endstanding 4-pyridines (ligands 1,4-bipyridyl-benzene and, 4,4-bipyridyl-biphenyl), but no bipyrimidine backbone.[18] That architecture is in strong contrast to the assembly of the mixture here, where no heteroleptic coordination networks were observed. Based on those prior experimental results or simply looking at the local environment around the Fe center, a heteroleptic mixture would be plausible. To understand the segregation behavior, one must consider what structure will be favorable for the overall thermodynamics of the system.

The drastic difference in the assembly behavior here (heteroleptic assembly vs. homoleptic segregation) can be attributed to the presence of the bipyrimidine chelate, which again accounts for the different stability of the homoleptic assemblies of endstanding bipyridines and bipyrimidine (PBP) ligands, respectively. While PBP forms a very stable coordination network on its own,[23] 1,4-bipyridyl-benzene
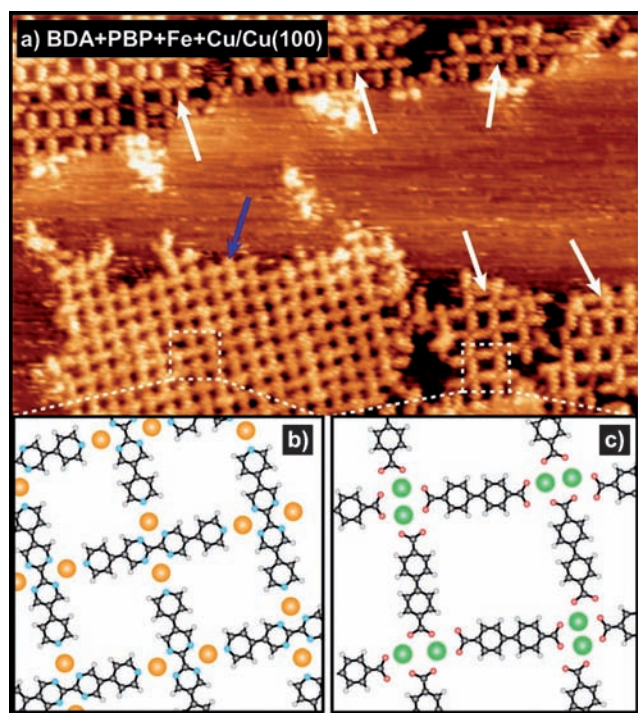
and 4,4-bipyridyl-biphenyl have only metastable homoleptic coordination alternatives on Cu(100)[19] and therefore are easier integrated into a heteroleptic coordination architecture.

From the point of view of systemic chemistry, the ligand mixture PBP, BDA, Cu, and Fe can be considered as a surface-confined programmed chemical system,[28] which enables subprogram processing of molecular information, here readout of coordination algorithms under confined conditions. In this sense, the pure Cu–PBP and Fe–BDA networks represent the linear readout of the binding information, while no evidence for a cross-over of the two ligand subroutines, for example, a mixed Fe–BDA–PBP phase, is observed.[29]

To further understand the emergence of Fe–BDA and Cu–PBP segregation, density functional theory (DFT) calculations were performed.[30] To model the electrostatics of the formed complexes under conditions near the metal surface, surface screening was modeled within the image charge model (see details of calculations in the Supporting Information). The observed segregation can effectively be explained by preferred stabilization of Fe^{II} by coordination of the deprotonated BDA ligand (under dimerization), while Cu^{I} is preferred by the neutral PBP ligand. Multiple combinations of the four components in this study were considered in the calculations. The calculations show that Cu bound to the BDA ligand is always energetically unfavorable (by at least 1.5 eV) when compared to the Fe^{II}–BDA combination. On the other hand, the formation of Fe^{II}–PBP would lead to a net $+4$ charge per unit cell; that charge is not likely to be stabilized by means of surface screening. Here, the electron charge transfer from the surface (owing to reported hybridization)[23] is instead expected to lead to Fe^{I}–PBP, a system within the same stability range as found for the Cu^{I}–PBP couple.

In Table 1, we summarize some of the results of the calculations for different possible combinations of binding units on Cu(100) that could be achieved with the available building blocks. More detail about these calculations is given in the Supporting Information. Table 1 compares three scenarios. The first is the interaction of Fe–BDA and a separate structure of Cu–PBP, which is the experimentally observed scenario. The second is the reverse combination: Fe–PBP binding and Cu–BDA binding, neither of which are observed in any control experiments. The third scenario is

a theoretically identified heteroleptic structure that combines all constituents (Cu, Fe, PBP, and BDA) within one network, as illustrated in the inset of Figure S2 in the Supporting Information. From Table 1 we see that DFT predicts that the first scenario is energetically favorable, consistent with the experimental result. Thus, parallel assembly of segregated homoleptic domains is the most stable system according to the DFT calculations.

Since STM measurements do not deliver direct chemical information of the adsorbates, the mismatching coordination pairs, BDA ligand with Cu atoms and PBP ligand with Fe atoms, were separately investigated as control experiments. In the first case, a pure molecular phase was formed without any evidence of the BDA molecules coordinating to Cu adatoms (Figure 2a, for further details see the Supporting Information).[25] Co-sublimation of the PBP/Fe pair on Ag(100) elucidates the coexistence of two distinct 2D phases: 1) a densely packed and well-ordered molecular phase of PBP

Figure 2. STM images of three control experiments. a) Self-assembled phase of BDA on Cu(100), with a molecular-model overlay (9.5 nm × 5.0 nm).[25] The carboxylate moieties do not interact with Cu adatoms. b) Self-assembly after deposition of PBP and Fe on Ag(100) at room temperature (image recorded at 5 K, 49 nm × 27.5 nm). Pure molecular PBP phase (blue arrow) coexists with unordered clusters (black arrow). c) Self-assembly of PBP and BDA on Cu(100) at room temperature after annealing at 450 K. BDA islands form the same structure as in (a; left side of image), while the PBP molecules coordinate with Cu adatoms, as observed previously[23] (32.5 nm × 11 nm).

Table 1: Calculated binding energies for three structural assemblies (DFT, see the Supporting Information for details).

Structure	Energy [eV]	Note
Fe^{II}–BDA and Cu^{I}–PBP	−11.9	experimentally observed selectivity[a]
Fe^{I}–PBP and Cu^{I}–BDA	−10.7	reversed pairing[b]
Fe^{II}–PBP–Cu^{I}–BDA	−9.2	bonding to produce mixed phase[b]

[a] This row corresponds to the experimentally observed segregation (Figure 1) and is found to be energetically favorable. [b] Second and third rows consider alternative possibilities: opposite metal segregation or a mixed phase (see Figure S2 in the Supporting Information).
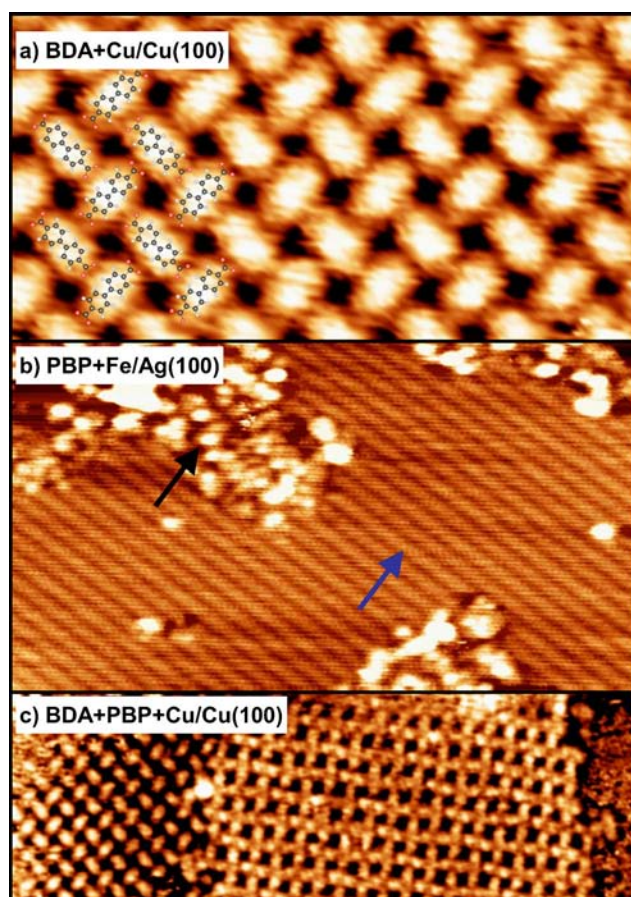
(rows indicated by blue arrow in Figure 2b) and 2) disordered Fe or Fe–PBP cluster agglomeration (black arrow in Figure 2b). This experiment was conducted on the Ag(100) surface to avoid the presence of Cu adatoms, which are present in a 2D lattice gas at room temperature on Cu(100).[31] Both the formation of pure PBP domains based on weak intermolecular interactions and of irregular iron clusters are in strong contrast to the outcome of the self-organization experiment of a PBP/Cu mixture on Ag(100) that generates a highly ordered PBP–Cu architecture, which is the same structure as observed herein on Cu(100) (for further details see the Supporting Information).[23] When no Fe is deposited on the surface, the annealing of the mixture of BDA and PBP ligands on Cu(100) at 450 K results in the pure BDA molecular phase and the Cu–PBP network phase, as shown in Figure 2c. Based on the behavior of the mismatching metal/ligand pairs, it can be concluded that copper centers in the PBP coordination network are not exchangeable with iron centers and the iron centers not with copper in the BDA coordination networks. In consequence, the molecular constituents that form the segregated supramolecular arrangements on the Cu(100) substrate can be unambiguously assigned from the STM data.

The coordinative interactions Cu–PBP and Fe–BDA are concluded here to be selective and thereby trigger segregation into two different metal–organic networks with quantitative yield. In the absence of the preferred coordination partner, weaker intermolecular interactions are preferred over complex formation with the mismatching metal species, thus emphasizing the highly selective character of the observed coordination motifs. Here, the network formation is purely steered by coordination bonding, in contrast to the many examples of cooperative assemblies (see introduction), where very flexible weak intermolecular interactions were involved.

In conclusion, we have shown that an instructed mixture of two ligands and two metal species, under surface-confinement, leads to selective assembly according to the coordination algorithms, thereby enabling the functionalization of surfaces with multiple independent supramolecular assemblies with distinct architectures and coordination chemistry. The systemic knowledge of how molecular components construct nano-architectures from complex, but instructed metal–ligand mixtures, sets the basis for establishing surface-confined coordination chemistry as an efficient, low-cost, bottom-up nanostructuring technique.

Experimental Section

The experiments were conducted in an ultra-high vacuum chamber (ca. 2×10^{-10} mbar) equipped with a home-built variable-temperature scanning tunneling microscope. The Cu(100) and Ag(100) samples were prepared by repeated cycles of sputtering with Ar$^+$ ions and annealing at 850 K. The molecular component BDA was purchased from Sigma–Aldrich (purity 97%), and PBP was synthesized following published protocols.[23] The molecular powders were sublimed from quartz crucibles at 490 and 465 K for BDA and PBP, respectively, resulting in about 8% of a monolayer (relative to the respective molecular phase). Subsequently the substrate was annealed to 450 K and atomic iron (purity 99.9%) was evaporated onto the hot substrate by using an electron beam evaporator. The STM topographs were acquired at 298 K, except for Figure 2b, which was recorded at 5 K.

[1] M. Böhringer, K. Morgenstern, W. D. Schneider, R. Berndt, F. Mauri, A. De Vita, R. Car, *Phys. Rev. Lett.* **1999**, *83*, 324–327.

[2] J. V. Barth, J. Weckesser, C. Z. Cai, P. Gunter, L. Burgi, O. Jeandupeux, K. Kern, *Angew. Chem.* **2000**, *112*, 1285; *Angew. Chem. Int. Ed.* **2000**, *39*, 1230.

[3] T. Yokoyama, S. Yokoyama, T. Kamikado, Y. Okuno, S. Mashiko, *Nature* **2001**, *413*, 619.

[4] A. Dmitriev, H. Spillmann, N. Lin, J. V. Barth, K. Kern, *Angew. Chem.* **2003**, *115*, 2774–2777; *Angew. Chem. Int. Ed.* **2003**, *42*, 2670–2673.

[5] J. Elemans, S. B. Lei, S. De Feyter, *Angew. Chem.* **2009**, *121*, 7434–7469; *Angew. Chem. Int. Ed.* **2009**, *48*, 7298–7332.

[6] L. Grill, M. Dyer, L. Lafferentz, M. Persson, M. V. Peters, S. Hecht, *Nat. Nanotechnol.* **2007**, *2*, 687–691.

[7] R. Gutzler, S. Lappe, K. Mahata, M. Schmittel, W. M. Heckl, M. Lackinger, *Chem. Commun.* **2009**, 680–682.

[8] R. Gutzler, H. Walch, G. Eder, S. Kloft, W. M. Heckl, M. Lackinger, *Chem. Commun.* **2009**, 4456–4458.

[9] L. Bartels, *Nat. Chem.* **2010**, *2*, 87.

[10] J. A. Theobald, N. S. Oxtoby, M. A. Phillips, N. R. Champness, P. H. Beton, *Nature* **2003**, *424*, 1029–1031.

[11] K. Tahara, S. Lei, W. Mamdouh, Y. Yamaguchi, T. Ichikawa, H. Uji-i, M. Sonoda, K. Hirose, F. C. De Schryver, S. De Feyter, Y. Tobe, *J. Am. Chem. Soc.* **2008**, *130*, 6666.

[12] K. G. Nath, O. Ivasenko, J. A. Miwa, H. Dang, J. D. Wuest, A. Nanci, D. F. Perepichka, F. Rosei, *J. Am. Chem. Soc.* **2006**, *128*, 4212–4213.

[13] S. Xu, M. Dong, E. Rauls, R. Otero, T. R. Linderoth, F. Besenbacher, *Nano Lett.* **2006**, *6*, 1434.

[14] L. Piot, C.-A. Palma, A. Llanes-Pallas, M. Prato, Z. Szekrényes, K. Kamarás, D. Bonifazi, P. Samorì, *Adv. Funct. Mater.* **2009**, *19*, 1207–1214.

[15] A. Langner, S. L. Tait, N. Lin, R. Chandrasekar, M. Ruben, K. Kern, *Angew. Chem.* **2008**, *120*, 8967–8970; *Angew. Chem. Int. Ed.* **2008**, *47*, 8835–8838.

[16] A. Langner, S. L. Tait, N. Lin, R. Chandrasekar, M. Ruben, K. Kern, *Chem. Commun.* **2009**, 2502–2504.

[17] J. Adisoejoso, K. Tahara, S. Okuhata, S. Lei, Y. Tobe, S. De Feyter, *Angew. Chem.* **2009**, *121*, 7489–7493; *Angew. Chem. Int. Ed.* **2009**, *48*, 7353–7357.

[18] A. Langner, S. L. Tait, N. Lin, C. Rajadurai, M. Ruben, K. Kern, *Proc. Natl. Acad. Sci. USA* **2007**, *104*, 17927–17930.

[19] S. L. Tait, A. Langner, N. Lin, S. Stepanow, C. Rajadurai, M. Ruben, K. Kern, *J. Phys. Chem. C* **2007**, *111*, 10982–10987.

[20] G. Pawin, K. L. Wong, D. Kim, D. Sun, L. Bartels, S. Hong, T. S. Rahman, R. Carp, M. Marsella, *Angew. Chem.* **2008**, *120*, 8570–8573; *Angew. Chem. Int. Ed.* **2008**, *47*, 8442–8445.

[21] S. Stepanow, T. Strunskus, M. Lingenfelder, A. Dmitriev, H. Spillmann, N. Lin, J. V. Barth, C. Woll, K. Kern, *J. Phys. Chem. B* **2004**, *108*, 19392–19397.

[22] C. C. Perry, S. Haq, B. G. Frederick, N. V. Richardson, *Surf. Sci.* **1998**, *409*, 512–520.

[23] S. L. Tait, A. Langner, N. Lin, R. Chandrasekar, O. Fuhr, M. Ruben, K. Kern, *ChemPhysChem* **2008**, *9*, 2495–2499.

[24] A. P. Seitsonen, M. Lingenfelder, H. Spillmann, A. Dmitriev, S. Stepanow, N. Lin, K. Kern, J. V. Barth, *J. Am. Chem. Soc.* **2006**, *128*, 5634–5635.

[25] S. Stepanow, N. Lin, J. V. Barth, K. Kern, *J. Phys. Chem. B* **2006**, *110*, 23472–23477.

[26] S. Clair, S. Pons, S. Fabris, S. Baroni, H. Brune, K. Kern, J. V. Barth, *J. Phys. Chem. B* **2006**, *110*, 5627–5632.

[27] N. Lin, S. Stepanow, F. Vidal, J. V. Barth, K. Kern, *Chem. Commun.* **2005**, 1681–1683.

[28] J. M. Lehn, *Science* **2002**, *295*, 2400–2403.

[29] J. M. Lehn, *Chem. Eur. J.* **2000**, *6*, 2097–2102.

[30] R. Ahlrichs, M. Bar, M. Haser, H. Horn, C. Kolmel, *Chem. Phys. Lett.* **1989**, *162*, 165–169.

[31] N. Lin, D. Payer, A. Dmitriev, T. Strunskus, C. Woll, J. V. Barth, K. Kern, *Angew. Chem.* **2005**, *117*, 1512; *Angew. Chem. Int. Ed.* **2005**, *44*, 1488.